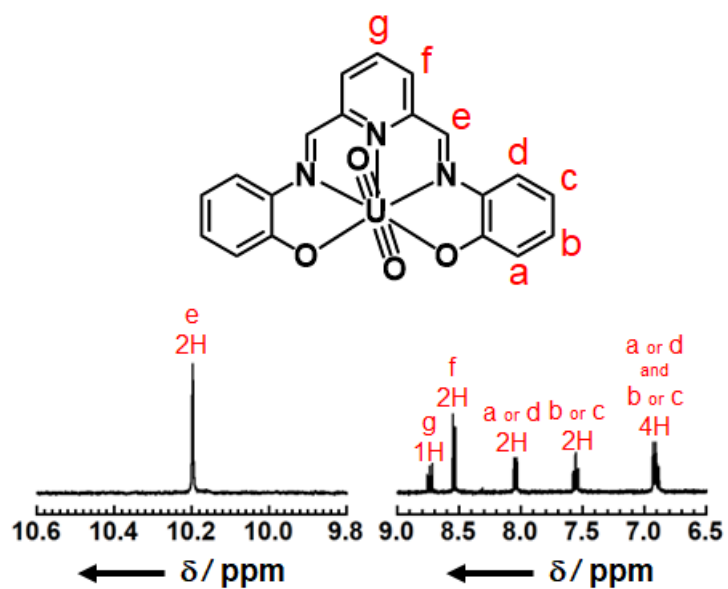


## Electronic Supplementary Information (ESI)

# Controlling Mixed-Valence States of Pyridyldiimino-bis(*o*-phenolato) Ligand Radical in Uranyl(VI) Complexes

Tomoyuki Takeyama, Satoru Tsushima, and Koichiro Takao



**Figure S1.**  $^1H$  NMR spectra of  $U^{VI}O_2(H,H\text{-pdiop})$  in  $DMSO-d_6$ .

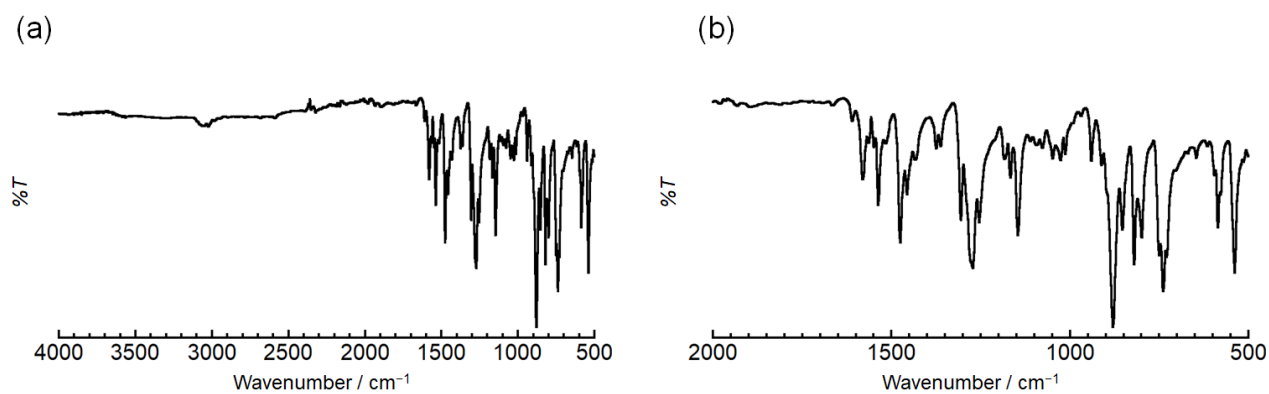


**Figure S2.** IR spectra of  $U^{VI}O_2(H,H\text{-pdiop})$ . Wavenumber regions: (a) 4000–500  $cm^{-1}$  and (b) 2000–500  $cm^{-1}$ .

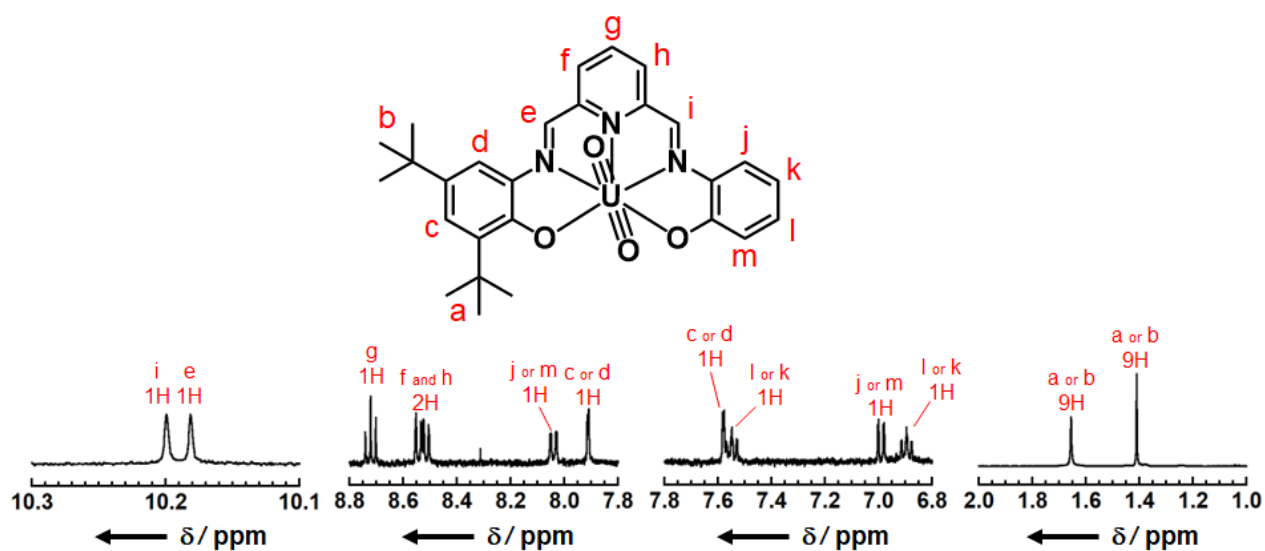


**Figure S3.**  $^1H$  NMR spectra of  $U^{VI}O_2(tBu,H-pdiop)$  in  $DMSO-d_6$ .

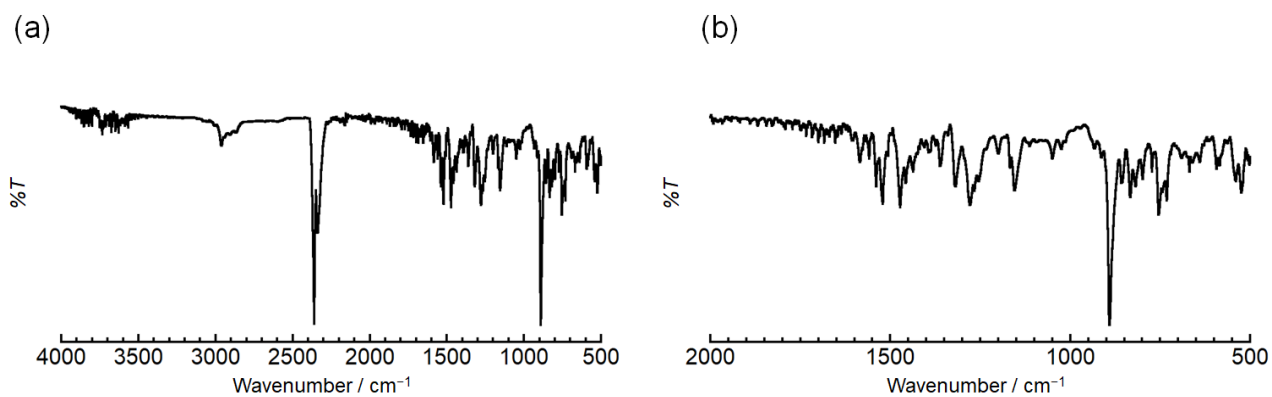


**Figure S4.** IR spectra of  $U^{VI}O_2(tBu,H-pdiop)$ . Wavenumber regions: (a) 4000–500  $cm^{-1}$  and (b) 2000–500  $cm^{-1}$ .

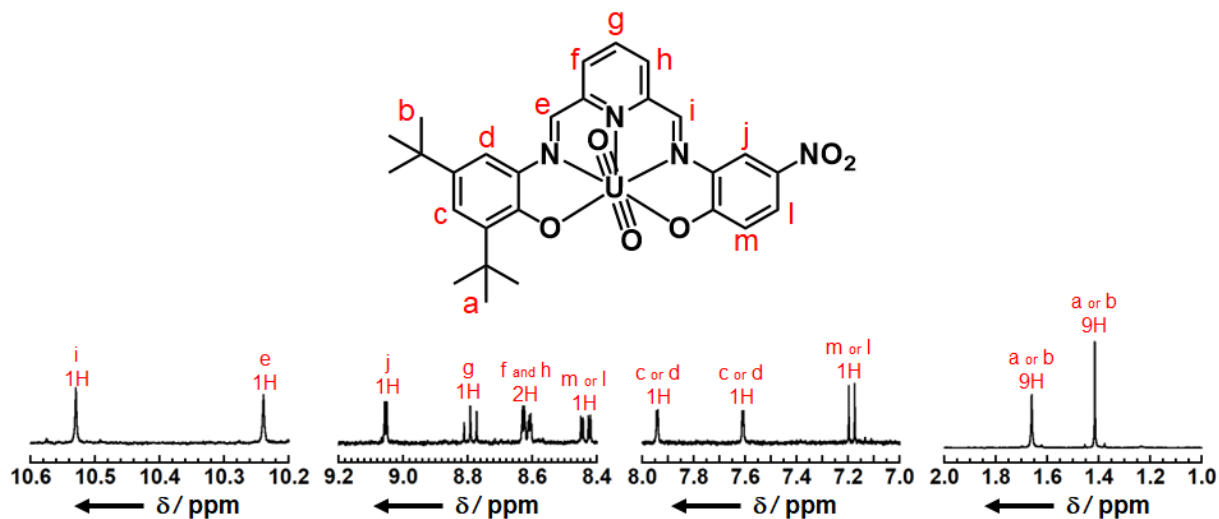


**Figure S5.**  $^1\text{H}$  NMR spectra of  $\text{U}^{\text{VI}}\text{O}_2(\text{tBu},\text{NO}_2\text{-pdiop})$  in  $\text{DMSO-}d_6$ .

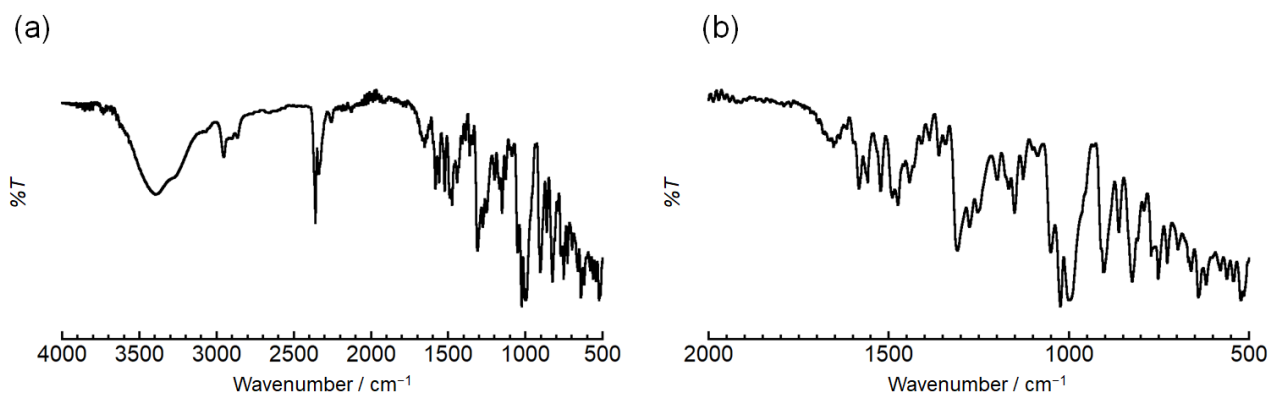


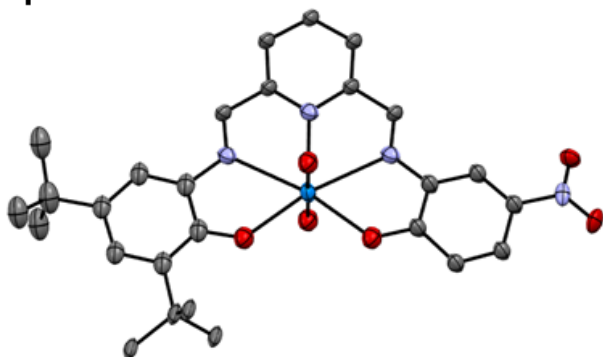
**Figure S6.** IR spectra of  $\text{U}^{\text{VI}}\text{O}_2(\text{tBu},\text{NO}_2\text{-pdiop})$ . Wavenumber regions: (a)  $4000\text{--}500\text{ cm}^{-1}$  and (b)  $2000\text{--}500\text{ cm}^{-1}$ .

**Table S1.** Selected bond lengths of the  $U^{VI}O_2(R_1,R_2\text{-pdiop})$  complexes based on the single crystal X-ray diffraction analyses.

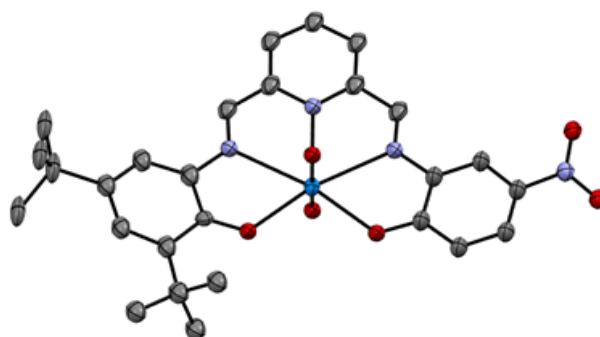
	H,H [Å]		tBu,H [Å]	tBu,NO <sub>2</sub> [Å]
U(1)–O(1)	1.784(8)	U(1)–O(1)	1.804(6)	1.75(4) <sup>a</sup>
		U(1)–O(2)	1.777(6)	1.80(7) <sup>a</sup>
U(1)–O(2)	2.274(8)	U(1)–O(3)	2.264(6)	2.30(2) <sup>a</sup>
		U(1)–O(4)	2.235(4)	2.25(1) <sup>a</sup>
U(1)–N(1)	2.551(10)	U(1)–N(1)	2.565(5)	2.56(2) <sup>a</sup>
		U(1)–N(3)	2.563(7)	2.53(3) <sup>a</sup>
U(1)–N(2)	2.557(13)	U(1)–N(2)	2.521(5)	2.56(2) <sup>a</sup>
C(7)–N(1)	1.323(16)	C(7)–N(1)	1.282(9)	1.27(2) <sup>a</sup>
		C(13)–N(3)	1.285(9)	1.29(2) <sup>a</sup>
C(1)–O(2)	1.325(14)	C(1)–O(3)	1.313(8)	1.30(2) <sup>a</sup>
		C(19)–O(4)	1.322(9)	1.32(4) <sup>a</sup>

<sup>a</sup> Average bond length of four independent molecules found in asymmetric units.

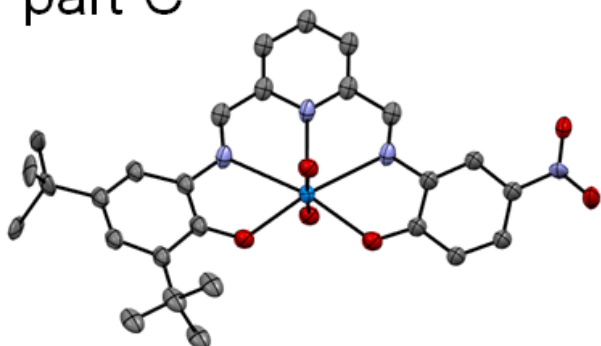
part A



part B



part C



part D

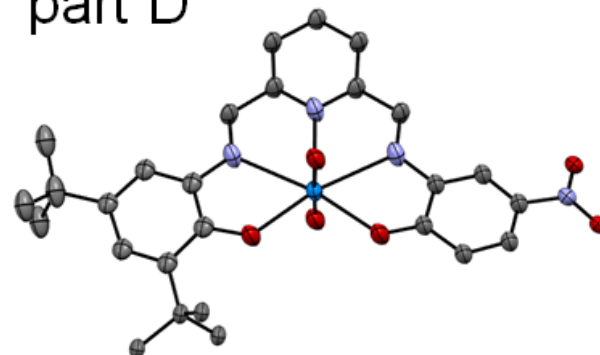


**Figure S7.** Molecular structures of  $U^{VI}O_2(tBu,NO_2\text{-pdiop})$  with thermal ellipsoids at 50% probability; hydrogen atoms and disordered atoms have been omitted for clarity.

### Detailed description of crystallographic analyses.

The single crystals of  $U^{VI}O_2(H,H\text{-pdiop})$  are obtained from DMSO/ethanol systems. Although the molecular structure of  $U^{VI}O_2(H,H\text{-pdiop})$  was obtained, some Alert level A and B are remained by check CIF report of International Union of Crystallography, as described below. The responses for these Alert are also described. To improve the large residual peaks of  $U^{VI}O_2(H,H\text{-pdiop})$ , we applied the numerical absorption correction by using indexed crystal faces. Even though, the large peaks remained. No better results have been obtained in use of the empirical absorption correction with strong absorber options. When any absorption correction was not applied, the  $R_{int}$  values increased, indicating that absorption correction should be done. Although we collected new data on a smaller crystal ( $0.15 \times 0.13 \times 0.05 \text{ mm}^3$ ), some Alert level A and B are remained. Despite these trials, the issue of residual peaks has not been resolved. Such an observation frequently occurs in a compound including a heavy atom.

\_vrf\_PLAT971\_210528\_uo2pdiop;

PROBLEM: Check Calcd Resid. Dens. 0.83Ang From U1 5.07 eA-3

PROBLEM: Check Calcd Resid. Dens. 0.77Ang From U1 3.34 eA-3

RESPONSE: We think that the insufficient or incorrect absorption correction is responsible of the residual densities. We applied the numerical absorption correction by using indexed crystal faces. Even though, the large peaks remained. No better results have been obtained in use of the empirical absorption correction with strong absorber options. Despite many trials, we cannot correct this issue. Such an observation is frequently occurred in the compounds including a heavy atom.

\_vrf\_PLAT972\_210528\_uo2pdiop;

PROBLEM: Check Calcd Resid. Dens. 1.22Ang From U1 -3.93 eA-3

RESPONSE: We think that the insufficient or incorrect absorption correction is responsible of the residual densities. We applied the numerical absorption correction by using indexed crystal faces.

Even though, the large peaks remained. No better results have been obtained in use of the empirical absorption correction with strong absorber options. Despite many trials, we cannot correct this issue. Such an observation is frequently occurred in the compounds including a heavy atom.

The single crystals of  $U^{VI}O_2(tBu,H-pdiop)$  are needle crystals obtained from  $CH_2Cl_2$ /hexane recrystallized systems. Moreover, it should be emphasized that its crystallinity readily drops after picking it up from the mother liquor, because crystalline solvents included in this compound easily evaporates to destroy the crystal structure. This reason would be volatilization of crystalline solvents. Any trials of recrystallization from other solvents with lower volatilities like pyridine and DMSO were unsuccessful. Therefore, we quickly mount a crystal on MiTeGen Dual Thickness MicroMounts, and set it on the temperature-controlled  $N_2$  gas flow (93 K), immediately to collect good diffraction data. In unit cell of  $U^{VI}O_2(tBu,H-pdiop)$ , some Q peaks and a solvent-accessible void were also observed. However, we could not find additional solvent molecules in the crystal structure, because these molecules would be heavily disordered. We tested SQUEEZE program and obtained a void of  $210 \text{ \AA}^3$  and 12 electrons per unit cell. This result implies that about 0.3  $CH_2Cl_2$  molecules exist in this crystal lattice. The presence of additional  $CH_2Cl_2$  is also confirmed by elemental analysis

In spite of many trials for recrystallization and SCXRD experiments, some Alert level A and B are remained by check CIF report of International Union of Crystallography, as described below. The responses for these Alert are also described. To improve the large residual peaks around U atoms of  $U^{VI}O_2(tBu,H-pdiop)$ , we applied the numerical absorption correction by using indexed crystal faces. Even though, the large peaks around U atoms remained. No better results have been obtained in use of the empirical absorption correction with strong absorber options. Despite these trials, the issue of residual peaks has not been resolved. Such an observation frequently occurs in a compound including a heavy atom.

\_vrf\_PLAT971\_tbuhpdiop\_mo\_3;

PROBLEM: Check Calcd Resid. Dens. 1.86Ang From C19 5.01 eA-3

PROBLEM: Check Calcd Resid. Dens. 0.79Ang From U1 3.15 eA-3

PROBLEM: Check Calcd Resid. Dens. 0.90Ang From U1 2.54 eA-3

RESPONSE: We think that the insufficient or incorrect absorption correction is responsible of the residual densities. We applied the numerical absorption correction by using indexed crystal faces. Even though, the large peaks remained. No better results have been obtained in use of the empirical absorption correction with strong absorber options. Despite many trials, we cannot correct this issue. Such an observation is frequently occurred in the compounds including a heavy atom.

\_vrf\_PLAT972\_tbuhpdiop\_mo\_3;

PROBLEM: Check Calcd Resid. Dens. 0.97Ang From U1 -2.71 eA-3

RESPONSE: We think that the insufficient or incorrect absorption correction is responsible of the residual densities. We applied the numerical absorption correction by using indexed crystal faces. Even though, the large peaks remained. No better results have been obtained in use of the empirical absorption correction with strong absorber options. Despite many trials, we cannot correct this issue. Such an observation is frequently occurred in the compounds including a heavy atom.

The single crystals of  $U^{VI}O_2(tBu,NO_2-pdiop)$  are tiny needle crystals obtained from pyridine/hexane recrystallized systems. Normally, a Mo  $K\alpha$  source is used for X-ray structural analysis of actinide complexes, but because the crystals are very thin, sufficient diffraction data could not be collected with Mo  $K\alpha$ . Here, we collected diffraction data for the crystal of  $U^{VI}O_2(tBu,NO_2-pdiop)$  using a Cu  $K\alpha$  source. Therefore, the absorption coefficient is rather large and some Alert level A and B are remained by check CIF report of International Union of Crystallography, as described below. The responses for these Alert are also described. To improve the large residual peaks around U atoms of  $U^{VI}O_2(tBu,NO_2-$

pdiop), we applied the numerical absorption correction by using indexed crystal faces. Even though, the large peaks around U atoms remained. No better results have been obtained in use of the empirical absorption correction with strong absorber options.

\_vrf\_PLAT342\_210628\_uo2tbuno2pdiop3

;

PROBLEM: Low Bond Precision on C-C Bonds ..... 0.03327 Ang.

RESPONSE: The investigated single crystal was a small-sized, brittle and poorly diffracting needle. Numerous datasets were collected on single crystals from different batches, whereof the one of the highest quality is reported herein. However, such low precision in bond lengths had to appear due to weak diffractions and disordering atomic locations.

\_vrf\_PLAT971\_210628\_uo2tbuno2pdiop3

;

PROBLEM: Check Calcd Resid. Dens. 0.91Ang From O1C 7.71 eA-3

PROBLEM: Check Calcd Resid. Dens. 0.76Ang From O2D 6.97 eA-3

PROBLEM: Check Calcd Resid. Dens. 0.81Ang From O1A 6.93 eA-3

PROBLEM: Check Calcd Resid. Dens. 0.64Ang From U1B 6.84 eA-3

PROBLEM: Check Calcd Resid. Dens. 0.80Ang From O2C 3.42 eA-3

PROBLEM: Check Calcd Resid. Dens. 0.95Ang From U1D 3.24 eA-3

PROBLEM: Check Calcd Resid. Dens. 0.77Ang From O2A 3.23 eA-3

PROBLEM: Check Calcd Resid. Dens. 0.70Ang From O1B 3.18 eA-3

PROBLEM: Check Calcd Resid. Dens. 0.22Ang From U1D 2.81 eA-3

RESPONSE: We think that the insufficient or incorrect absorption correction is responsible of the residual densities. We applied the numerical absorption correction by using indexed crystal faces. Even though, the large peaks remained. No better results have been obtained in use of the empirical

absorption correction with strong absorber options. Despite many trials, we cannot correct this issue. Such an observation is frequently occurred in the compounds including a heavy atom.

;

\_vrf\_PLAT972\_210628\_uo2tbuno2pdio3

;

PROBLEM: Check Calcd Resid. Dens. 1.01Ang From U1C -6.16 eA-3

PROBLEM: Check Calcd Resid. Dens. 1.09Ang From U1D -5.45 eA-3

PROBLEM: Check Calcd Resid. Dens. 0.96Ang From U1B -5.43 eA-3

PROBLEM: Check Calcd Resid. Dens. 0.87Ang From U1A -5.32 eA-3

PROBLEM: Check Calcd Resid. Dens. 0.94Ang From U1C -4.68 eA-3

PROBLEM: Check Calcd Resid. Dens. 0.92Ang From U1D -4.64 eA-3

PROBLEM: Check Calcd Resid. Dens. 1.06Ang From U1A -4.31 eA-3

PROBLEM: Check Calcd Resid. Dens. 1.05Ang From U1B -4.22 eA-3

PROBLEM: Check Calcd Resid. Dens. 0.81Ang From U1D -3.73 eA-3

PROBLEM: Check Calcd Resid. Dens. 0.93Ang From U1A -3.34 eA-3

PROBLEM: Check Calcd Resid. Dens. 0.91Ang From U1B -3.18 eA-3

PROBLEM: Check Calcd Resid. Dens. 0.77Ang From U1B -3.03 eA-3

PROBLEM: Check Calcd Resid. Dens. 0.84Ang From U1A -2.88 eA-3

PROBLEM: Check Calcd Resid. Dens. 0.92Ang From U1B -2.85 eA-3

PROBLEM: Check Calcd Resid. Dens. 0.83Ang From U1A -2.75 eA-3

PROBLEM: Check Calcd Resid. Dens. 0.81Ang From U1C -2.72 eA-3

PROBLEM: Check Calcd Resid. Dens. 0.84Ang From U1D -2.60 eA-3

RESPONSE: We think that the insufficient or incorrect absorption correction is responsible of the residual densities. We applied the numerical absorption correction by using indexed crystal faces. Even though, the large peaks remained. No better results have been obtained in use of the empirical

absorption correction with strong absorber options. Despite many trials, we cannot correct this issue. Such an observation is frequently occurred in the compounds including a heavy atom.

;

\_vrf\_PLAT973\_210628\_uo2tbuno2pdiop3

;

PROBLEM: Check Calcd Positive Resid. Density on U1A 3.75 eA-3

PROBLEM: Check Calcd Positive Resid. Density on U1C 3.36 eA-3

PROBLEM: Calcd Positive Resid. Density on U1B 3.33 eA-3

RESPONSE: We think that the insufficient or incorrect absorption correction is responsible of the residual densities. We applied the numerical absorption correction by using indexed crystal faces. Even though, the large peaks remained. No better results have been obtained in use of the empirical absorption correction with strong absorber options. Despite many trials, we cannot correct this issue. Such an observation is frequently occurred in the compounds including a heavy atom.

;

\_vrf\_PLAT975\_210628\_uo2tbuno2pdiop3

;

PROBLEM: Check Calcd Resid. Dens. 0.78Ang From O2D . 1.60 eA-3

PROBLEM: Check Calcd Resid. Dens. 0.89Ang From O2B . 1.59 eA-3

RESPONSE: We think that the insufficient or incorrect absorption correction is responsible of the residual densities. We applied the numerical absorption correction by using indexed crystal faces. Even though, the large peaks remained. No better results have been obtained in use of the empirical absorption correction with strong absorber options. Despite many trials, we cannot correct this issue. Such an observation is frequently occurred in the compounds including a heavy atom.

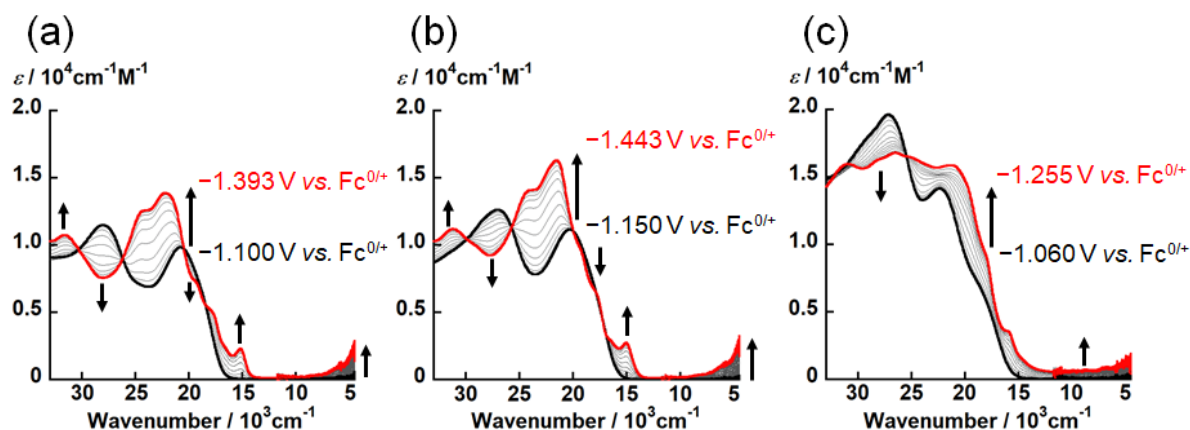


**Figure S8.** UV-vis-NIR spectral change of electrochemical reduction of  $\text{U}^{\text{VI}}\text{O}_2(\text{H,H-pdiop})$  (a),  $\text{U}^{\text{VI}}\text{O}_2(\text{tBu,H-pdiop})$  (b) and  $\text{U}^{\text{VI}}\text{O}_2(\text{tBu,NO}_2\text{-pdiop})$  (c). recorded at different applied potentials (potential step: 15 or 20 mV) in DMSO with 0.1 M TBAP at 295 K. Black and red bold curves represent absorption spectra of the parent  $\text{U}^{\text{VI}}\text{O}_2^{2+}$  complexes and their singly-reduced complexes, respectively.

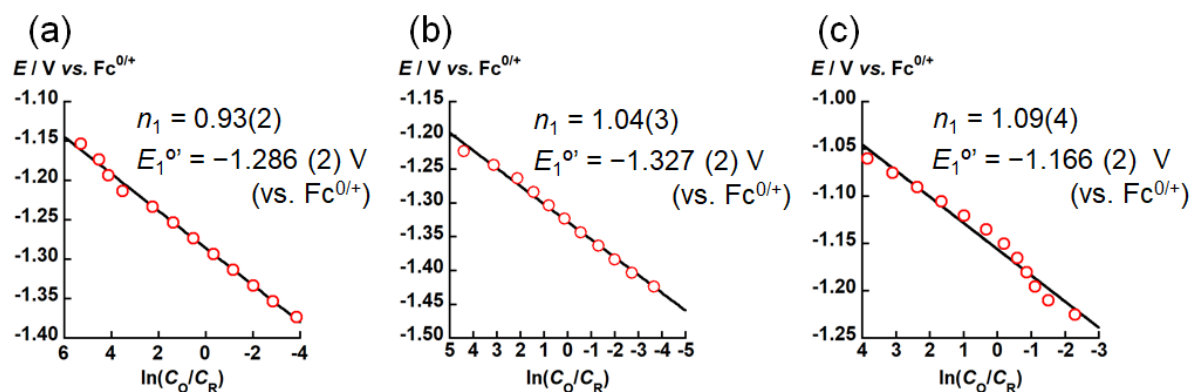


**Figure S9.** Nernstian plot for the spectral change of the electrochemical reduction of  $\text{U}^{\text{VI}}\text{O}_2(\text{H,H-pdiop})$  (a),  $\text{U}^{\text{VI}}\text{O}_2(\text{tBu,H-pdiop})$  (b) and  $\text{U}^{\text{VI}}\text{O}_2(\text{tBu,NO}_2\text{-pdiop})$  (c). The  $C_{\text{O}}/C_{\text{R}}$  was calculated from the absorbance at  $22272\text{ cm}^{-1}$  (a),  $21552\text{ cm}^{-1}$  (b) and  $21637\text{ cm}^{-1}$  (c).

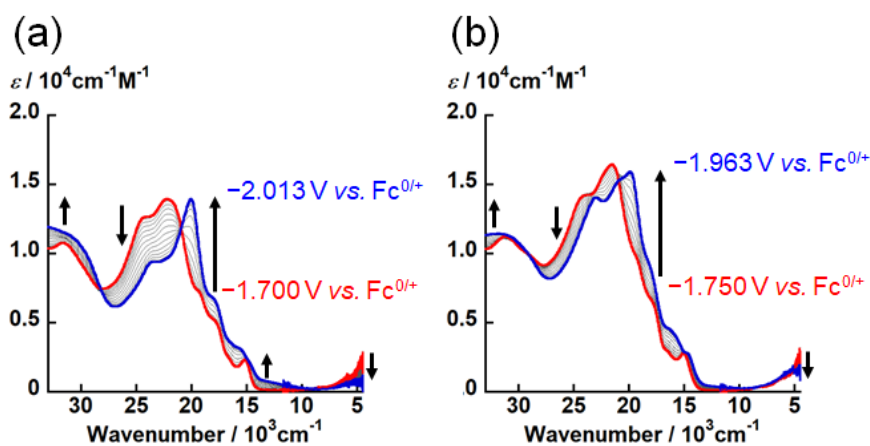


**Figure S10.** UV-vis-NIR spectral change of electrochemical reduction of  $[\text{UO}_2(\text{H,H-pdiop})]^-$  (a) and  $[\text{UO}_2(\text{tBu,H-pdiop})]^-$  (b) recorded at different applied potentials (potential step: 15 or 20 mV) in DMSO with 0.1 M TBAP at 295 K. Red and blue bold curves represent absorption spectra of the singly-reduced complexes and the doubly-reduced complexes.

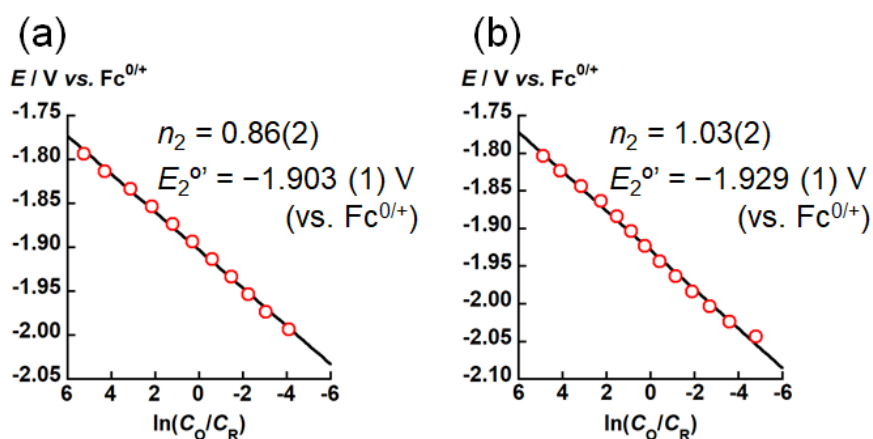


**Figure S11.** Nernstian plot for the spectral change of the electrochemical reduction of  $[\text{UO}_2(\text{H,H-pdiop})]^-$  (a) and  $[\text{UO}_2(\text{tBu,H-pdiop})]^-$  (b). The  $C_O/C_R$  was calculated from the absorbance at  $20534 \text{ cm}^{-1}$  (a) and  $19881 \text{ cm}^{-1}$  (b).

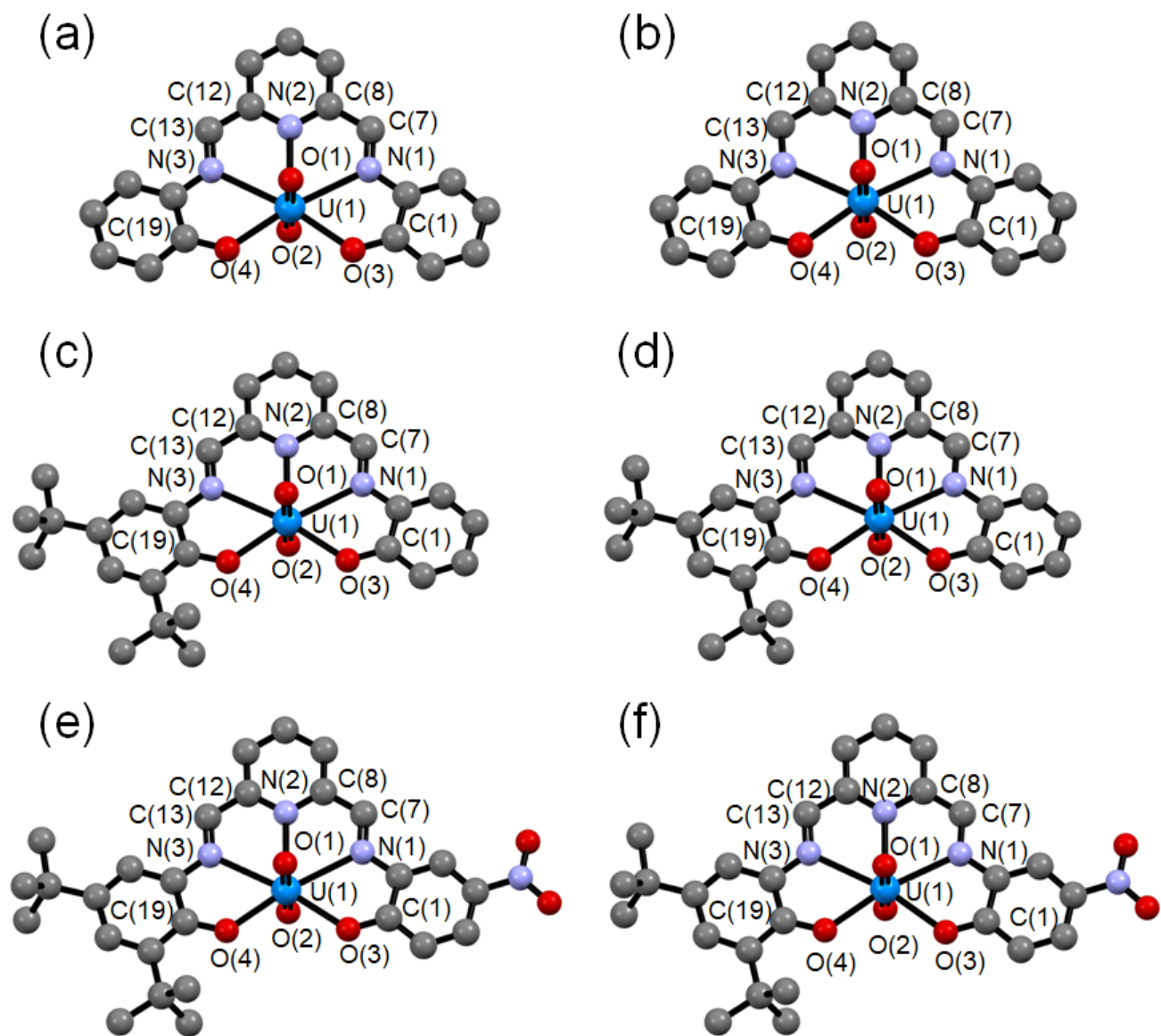


**Figure S12.** DFT-optimized structures of  $U^{VI}O_2(H,H\text{-pdio})$  (a),  $[UO_2(H,H\text{-pdio})]^-$  (b),  $U^{VI}O_2(tBu,H\text{-pdio})$  (c),  $[UO_2(tBu,H\text{-pdio})]^-$  (d),  $U^{VI}O_2(tBu,NO_2\text{-pdio})$  (e), and  $[UO_2(tBu,NO_2\text{-pdio})]^-$  (f).

**Table S2.** Selected Bond Lengths (Å) of DFT-optimized structures of  $[\text{UO}_2(\text{H},\text{H-pdiop})]^{-/0}$ ,  $[\text{UO}_2(\text{tBu},\text{H-pdiop})]^{-/0}$  and  $[\text{UO}_2(\text{tBu},\text{NO}_2\text{-pdiop})]^{-/0}$ .

	$\text{U}^{\text{VI}}\text{O}_2(\text{H},\text{H-pdiop})$	$[\text{UO}_2(\text{H},\text{H-pdiop})]^-$	$\text{U}^{\text{VI}}\text{O}_2(\text{tBu},\text{H-pdiop})$	$[\text{UO}_2(\text{tBu},\text{H-pdiop})]^-$	$\text{U}^{\text{VI}}\text{O}_2(\text{tBu},\text{NO}_2\text{-pdiop})$	$[\text{UO}_2(\text{tBu},\text{NO}_2\text{-pdiop})]^-$
U(1)–O(1)	1.789	1.801	1.790	1.802	1.787	1.797
U(1)–O(2)	1.789	1.801	1.790	1.802	1.787	1.797
U(1)–O(3)	2.311	2.325	2.306	2.314	2.333	2.350
U(1)–O(4)	2.312	2.325	2.298	2.316	2.271	2.298
U(1)–N(1)	2.638	2.594	2.640	2.578	2.650	2.563
U(1)–N(2)	2.600	2.525	2.591	2.530	2.600	2.541
U(1)–N(3)	2.638	2.596	2.625	2.614	2.628	2.625
C(7)–N(1)	1.288	1.311	1.288	1.324	1.284	1.333
C(7)–C(8)	1.456	1.428	1.456	1.417	1.458	1.412
C(8)–N(2)	1.349	1.376	1.349	1.380	1.349	1.377
C(12)–N(2)	1.349	1.376	1.349	1.369	1.348	1.362
C(12)–C(13)	1.456	1.428	1.455	1.441	1.455	1.449
C(13)–N(3)	1.288	1.311	1.290	1.300	1.289	1.293

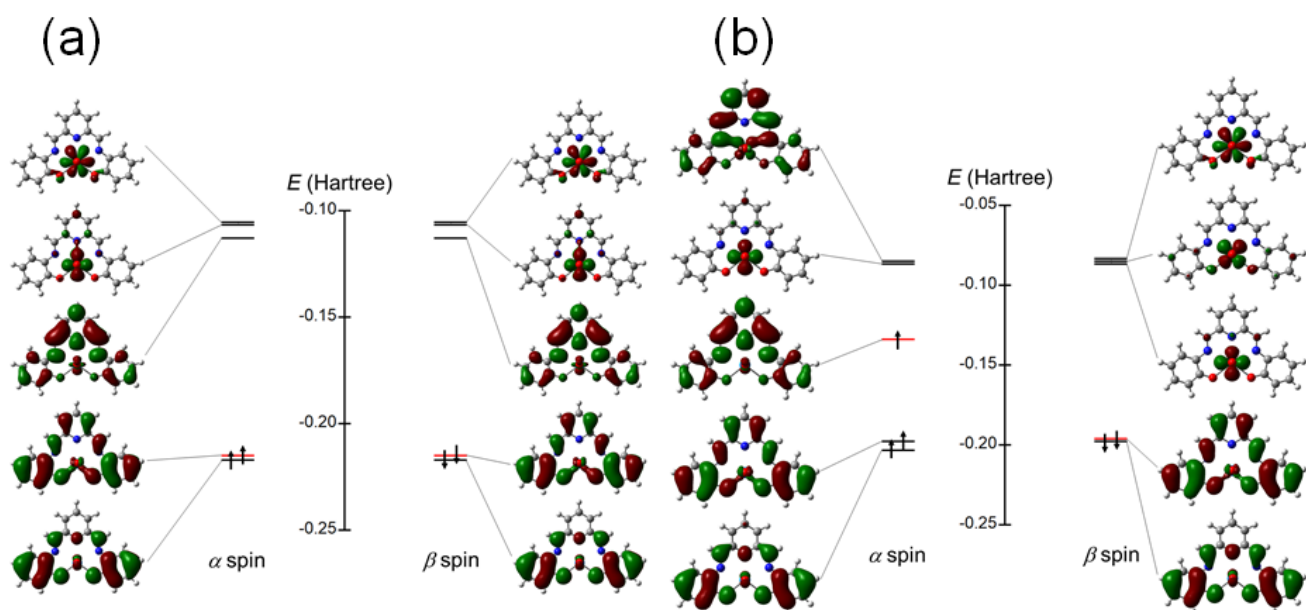


**Figure S13.** Calculated MO energy diagrams of  $U^{VI}O_2(H,H-pdiop)$  (a) and  $[UO_2(H,H-pdiop^{*3-})]^-$  (b).

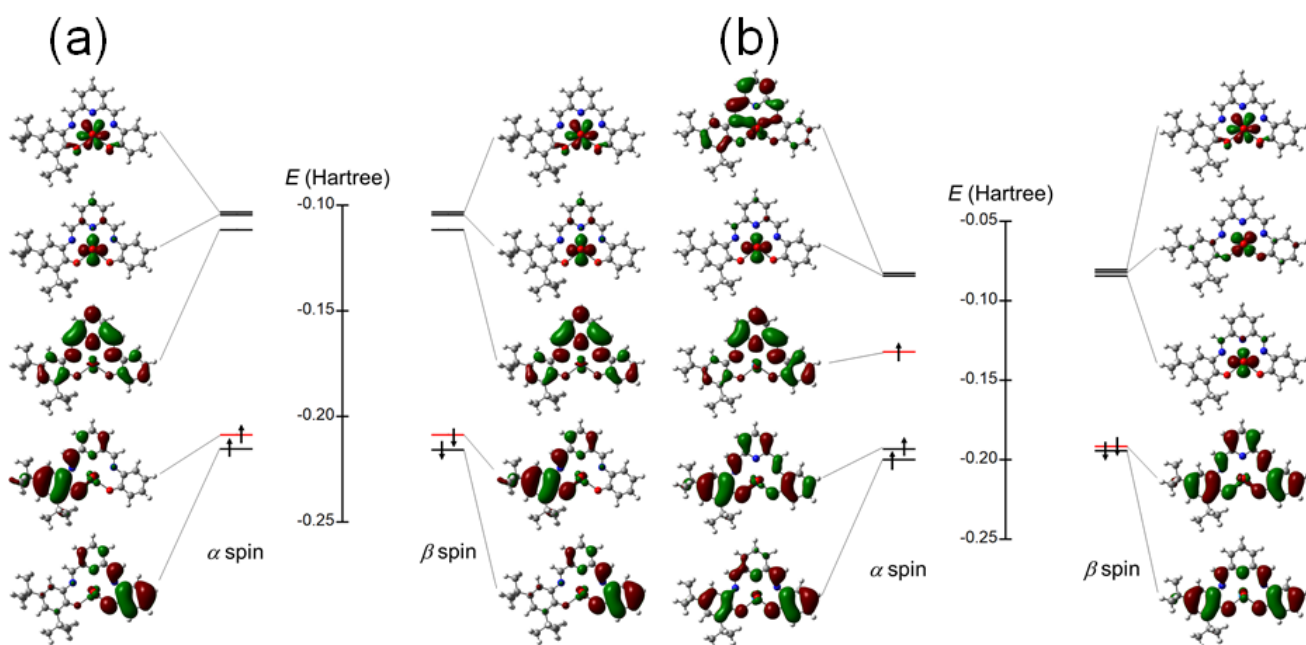


**Figure S14.** Calculated MO energy diagrams of  $U^{VI}O_2(tBu,H-pdiop)$  (a) and  $[UO_2(tBu,H-pdiop^{*3-})]^-$  (b).

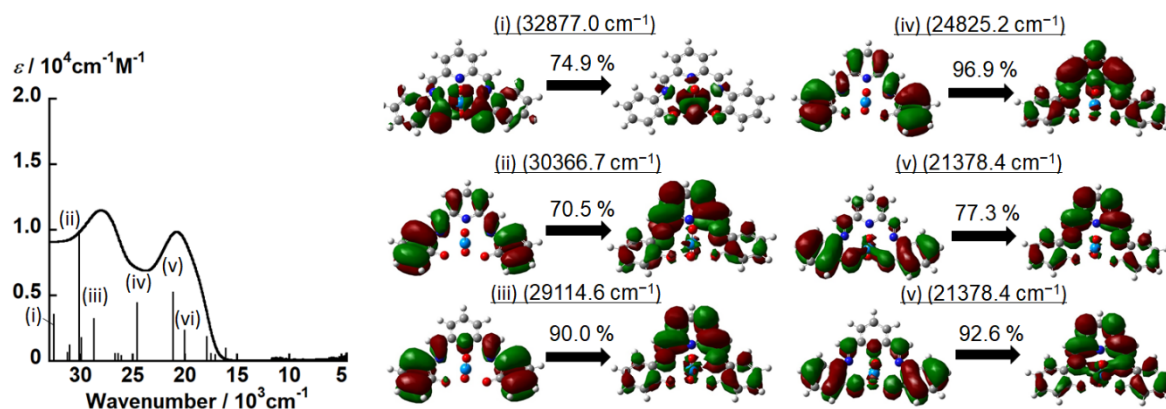


**Figure S15.** UV-vis-NIR spectrum of  $\text{U}^{\text{VI}}\text{O}_2(\text{H,H-pdiop})$  in DMSO and predicted band positions and intensities of the TD-DFT calculation. The vertical black lines correspond to the calculated transitions for  $\text{U}^{\text{VI}}\text{O}_2(\text{H,H-pdiop})$ .

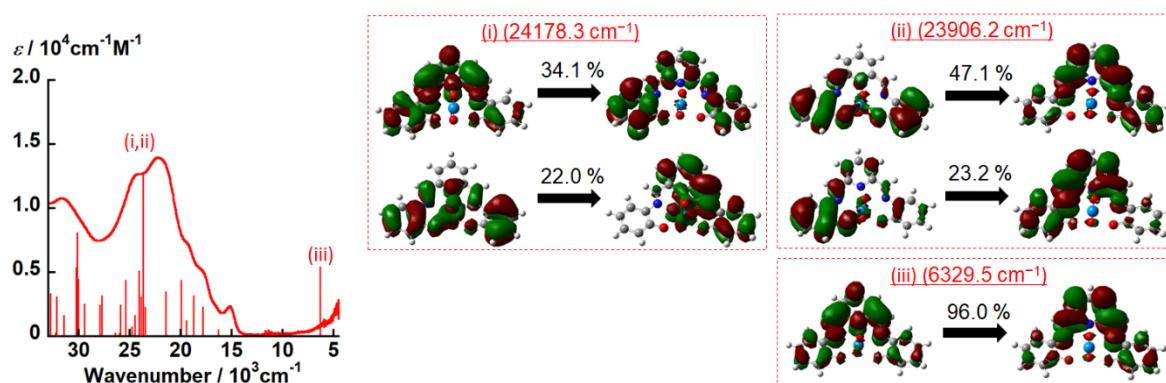


**Figure S16.** UV-vis-NIR spectrum of  $[\text{UO}_2(\text{H,H-pdiop})]^-$  in DMSO and predicted band positions and intensities of the TD-DFT calculation. The vertical red lines correspond to the calculated transitions for  $[\text{UO}_2(\text{H,H-pdiop})]^-$ .

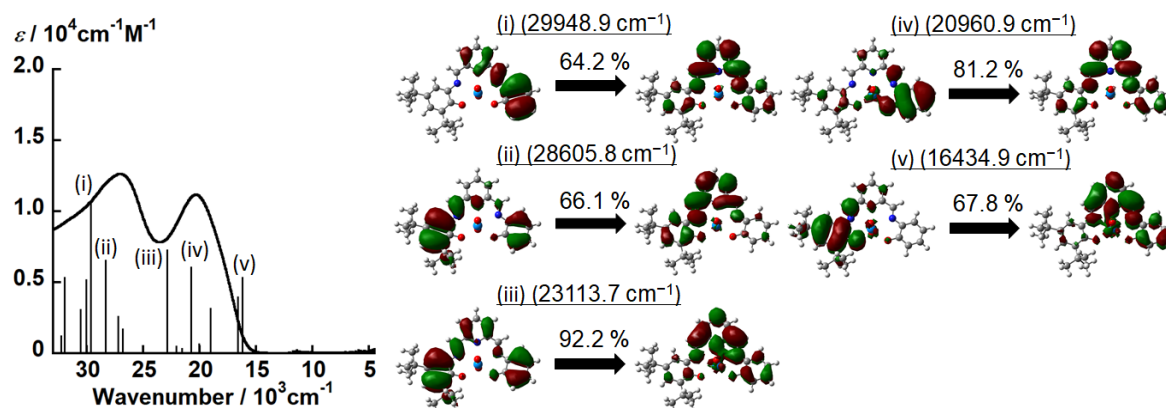


**Figure S17.** UV-vis-NIR spectrum of  $\text{U}^{\text{VI}}\text{O}_2(\text{tBu,H-pdiop})$  in DMSO and predicted band positions and intensities of the TD-DFT calculation. The vertical black lines correspond to the calculated transitions for  $\text{U}^{\text{VI}}\text{O}_2(\text{tBu,H-pdiop})$ .

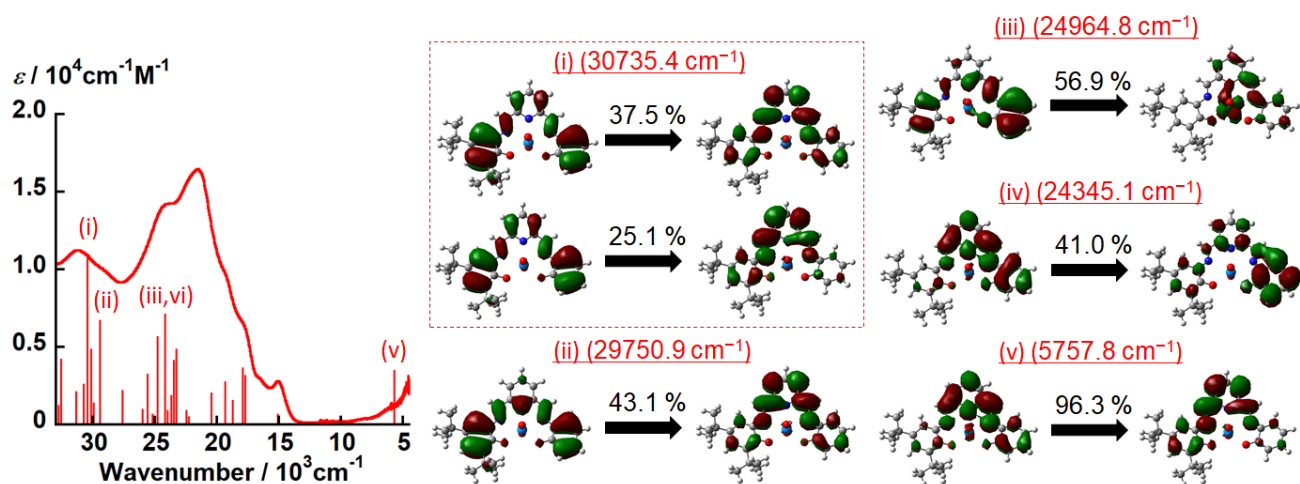


**Figure S18.** UV-vis-NIR spectrum of  $[\text{UO}_2(\text{tBu,H-pdiop})]^-$  in DMSO and predicted band positions and intensities of the TD-DFT calculation. The vertical red lines correspond to the calculated transitions for  $[\text{U}^{\text{VI}}\text{O}_2(\text{tBu,H-pdiop})]^-$ .

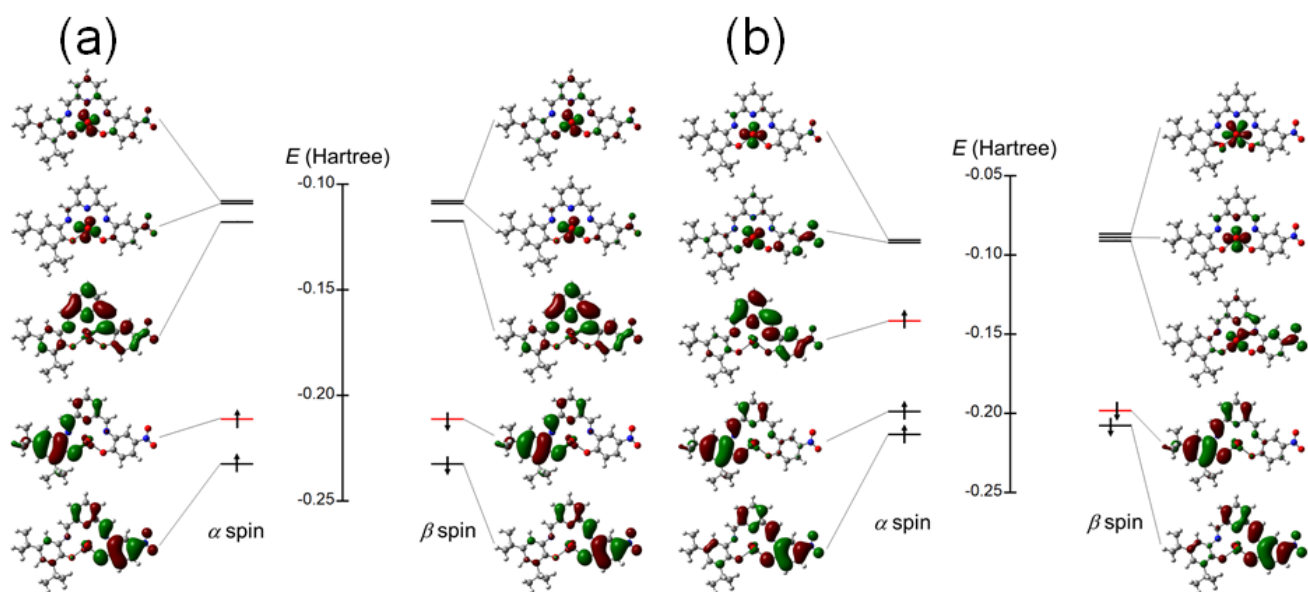


**Figure S19.** Calculated MO energy diagrams of  $\text{U}^{\text{VI}}\text{O}_2(\text{tBu,NO}_2\text{-pdiop})$  (a) and  $[\text{UO}_2(\text{tBu,NO}_2\text{-pdiop})]^-$  (b).

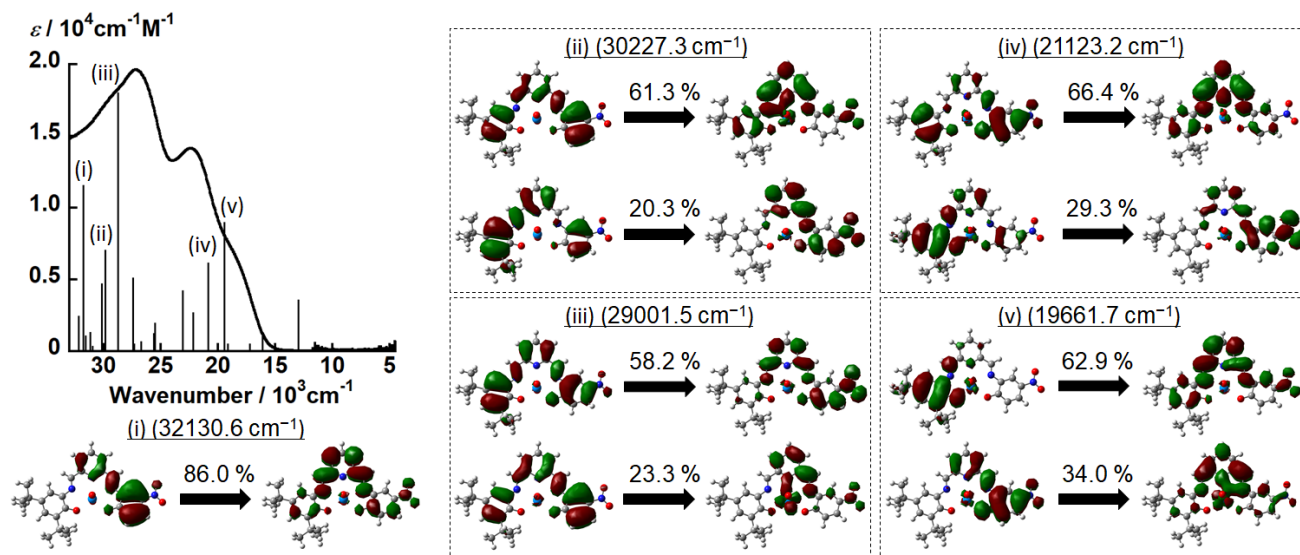


**Figure S20.** UV-vis-NIR spectrum of  $U^{VI}O_2(tBu,NO_2-pdiop)$  in DMSO and predicted band positions and intensities of the TD-DFT calculation. The vertical black lines correspond to the calculated transitions for  $U^{VI}O_2(tBu,NO_2-pdiop)$ .

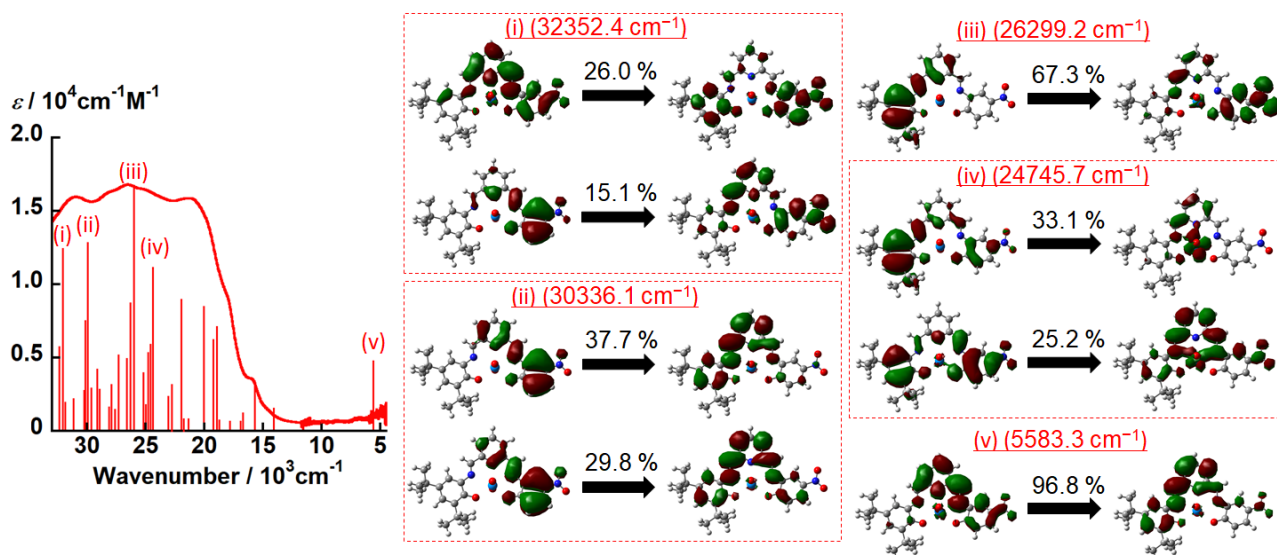


**Figure S21.** UV-vis-NIR spectrum of  $[UO_2(tBu,NO_2-pdiop)]^-$  in DMSO and predicted band positions and intensities of the TD-DFT calculation. The vertical red lines correspond to the calculated transitions for  $[UO_2(tBu,NO_2-pdiop)]^-$ .